Polymer Vol. 37 No. 12, pp. 2385–2394, 1996

0032-3861/96/$15.00+0.00

Single-phase and multiple-phase thermoplastic/thermoset polyblends: 2. Morphologies and mechanical properties of phenoxy/epoxy blends

Kun-Chun Teng and Feng-Chih Chang*
Institute of Applied Chemistry, National Chiao-Tung University, Hsinchu, Taiwan, Republic of China
(Received 22 May 1995; revised 24 August 1995)

Homogeneous and inhomogeneous phenoxy/epoxy blends can be prepared by kinetic control of the curing rate. Spinodal decomposition is the dominant phase separation mechanism of the inhomogeneous blends. A considerable fraction of the added phenoxy is dissolved in the epoxy matrix of each inhomogeneous blend and the intrinsic properties of the epoxy matrix are changed in the blend. The intrinsic toughness of the epoxy increases on increasing the amount of dissolved phenoxy. The homogeneous blend that has the highest content of dissolved phenoxy also possesses the highest fracture toughness. A crack-blunting mechanism, namely a localized shear plastic deformation around the crack tip region prior to the onset of crack growth, has been used to explain the fracture behaviour seen in this study. The degree of blunting caused by shear yielding is the most important factor in controlling the subsequent mode of crack growth and the fracture toughness. Copyright © 1996 Elsevier Science Ltd.

(Keywords: epoxy; phenoxy; blend)

INTRODUCTION

The fracture behaviour of crosslinked epoxy networks is significantly different from that of linear thermoplastics and different approaches have been utilized to toughen these two classes of polymers. Liquid rubbers such as amino- and carboxy-terminated butadiene–acrylonitrile rubbers (ATBNs and CTBNs) have been successfully applied in toughening numerous epoxy resins. These liquid rubbers are usually dissolved in the precured epoxy monomer (with the curing agent) and then precipitated later to form a second rubber phase during the curing process. The rubber modification of the epoxy resin leads to an increase in the epoxy toughness of more than an order of magnitude, but this increase in toughness is invariably accompanied by a reduction in modulus and glass transition temperature.

Toughening of highly crosslinked epoxy resins by blending with various thermoplastics has drawn great interest lately. In general, the toughness improvement achieved by blending with high T_g thermoplastics is less marked than that achieved using conventional liquid rubbers. However, the disadvantages resulting from liquid rubbers, such as lower modulus and T_g, can be eliminated. Toughening epoxies using various thermoplastics has been the subject of a recent review[1]. Bucknall and coworkers[2–5] were probably the first to initiate this interesting area of study by blending polyethersulfone (PES) with epoxy resin networks. Since then, various PES/epoxy blends have been further investigated by several others[6–13]. Other thermoplastics such as polyetherimide (PEI)[14–20], poly(phenyl oxide) (PPO)[21–23], poly(butylene terephthalate) (PBT)[24–26], nylons[24,25,27], polyurethane[28,29], polycarbonate[30], phenoxy resin[31], poly(aryl ether ketone)s[32], poly(methyl methacrylate)[33], polyimide[34] and many others[35–37] have also been used to toughen various epoxy resins. With only a few exceptions[24,25,27], most of the above-mentioned examples involved a process of dissolving the thermoplastic in the precured epoxy monomer (with the curing agent) prior to curing and allowing phase separation to occur to different degrees. In a few cases, single-phase blends were obtained when low molecular weight thermoplastics were employed[10,32,35].

Our approach to studying thermoplastic/epoxy blends is somewhat different from most prior studies in placing emphasis on the kinetic control of the blend morphologies by varying the amount of accelerator. At present, we are able to control kinetically the blend morphologies, either as single-phase or multiple-phase blends, for three different systems: phenoxy/epoxy[31], PEI/epoxy[18] and thermoplastic polyurethane (TPU)/epoxy[29]. In the first paper of this series[31], we reported the kinetics and mechanism of formation for the phenoxy/epoxy system. Cured products that are opaque, translucent or transparent can be obtained by kinetic control of the curing rate. Phenoxy is miscible with epoxy monomer and the low molecular weight epoxy resin during the early stages

* To whom correspondence should be addressed

of curing, but tends to separate out when the epoxy resin molecular weight has increased to a critical value (thermodynamically immiscible). Phase separation now becomes a kinetically controlled diffusion process, and the mixture viscosity increases to a critical level where the diffusion process is difficult or completely impossible. Therefore, the degree of phase separation of the finally cured product depends on the curing rate during this critical time period. This paper will present additional information on the rate-controlled morphologies and the related mechanical properties of the phenoxy/epoxy blends.

EXPERIMENTAL

Liquid epoxy resin Epon 826 (epoxid equivalent weight, $EEW = 182$) was obtained from Shell. Phenoxy resin PHKK, a high molecular weight ($M_w = 20\,000$–$25\,000\,g\,mol^{-1}$) thermoplastic made from bisphenol-A and epichlorohydrin, was obtained from Union Carbide. Diaminodiphenyl sulfone (DDS) and 1-cyanoethyl-2-ethyl-4-methylimidazole (CEMI) were respectively the curing agent and accelerator employed in this study.

Powdered phenoxy resin (10 phr) was dissolved in the epoxy monomer at 110°C and a stoichiometric amount of the curing agent was added. The mixture was then degassed at 100°C in a vacuum oven for approximately 15 min. The resultant clear solution was then cooled at 70°C, the desired quantity of accelerator was added and the mixture was cast immediately into a Teflon die. The curing sequence involved heating at 135°C for 1.5 h, 160°C for 1.5 h and 190°C for an additional 2.5 h.

The percentage transmittance at 650 nm of each cured specimen was measured using a Hitachi 330 photospectrometer. Dynamic viscoelastic properties of the cured specimens were measured using a Rheometrics RDS-II between 25 and 250°C at 3°C per step, $10\,rad\,s^{-1}$ and 0.1% strain. Tensile breaking strength and modulus were measured with a strain gauge according to ASTM D683-86 Type-I at a testing rate of $5\,mm\,min^{-1}$ using an Instron machine. The compressive yield stress was measured according to ASTM D695 with cylinder-type specimens ($D = 11$ mm, $H = 22$ mm) using an MTS 810. The nominal strain (e) was determined from the crosshead displacement, corrected for machine softness. The load (P) was converted into true stress (σ_t) using the initial cross-sectional area (A_0) and

$$\sigma_t = P(1 - e)/A_0 \quad (1)$$

which was derived by assuming constant volume deformation.

The fracture toughness, or stress intensity factor (K_{IC}), values were obtained according to ASTM E399-83. The compact tension specimens measured approximately $50 \times 40 \times 10$ mm, and in each specimen a sharp crack was formed at the base of the slot by carefully tapping a fresh razor blade into the base for a short distance. The testing was carried out at a constant displacement rate of $2.0\,mm\,min^{-1}$. The value of the stress intensity factor (K_{IC}) was calculated from

$$K_{IC} = \frac{P_{max}}{BW^{1/2}} f(a/W) \quad (2)$$

where

$$f(a/W) = \frac{(2 + a/W)(0.886 + 4.64a/W - 13.32a^2/W^2 + 14.72a^3/W^3 - 5.6a^4/W^4)}{(1 - a/W)^{3/2}} \quad (3)$$

where P_{max} is the maximum load, B is the specimen thickness, a is the crack length, W is the width of the specimen and $f(a/W)$ is the geometric factor. The corresponding fracture energy (G_{IC}) values were obtained from K_{IC} using

$$G_{IC} = \frac{K_{IC}^2}{E}(1 - \nu^2) \quad (4)$$

where Poisson's ratio (ν) was taken as 0.4 for all materials.

RESULTS AND DISCUSSION

Morphologies observed through scanning electron microscopy (SEM)

Table 1 summarizes the relationship between the amount of accelerator, gel time, transmittance and T_g for the phenoxy/epoxy blends. *Figure 1* contains the SEM micrographs of the solvent-etched blends and

Table 1 Summarized data of the blends

Blend	Transmittance (%)	Gel time (min)	Density ($g\,cm^{-3}$)	T_g by RDS[a] (°C)	
				Phenoxy	Epoxy
Phenoxy			1.170	93	
Epoxy/DDS	89		1.243		194
Phenoxy/epoxy/DDS (0 phr CEMI)	0	72	1.229	89	189
Phenoxy/epoxy/DDS (0.1 phr CEMI)	7	62	1.223	92	190
Phenoxy/epoxy/DDS (0.15 phr CEMI)	34	46	1.234	104	189
Phenoxy/epoxy/DDS (0.3 phr CEMI)	83	24	1.235		184
Phenoxy/epoxy/DDS (0.5 phr CEMI)	87	6	1.237		178

[a] Rheometric dynamic spectrometry

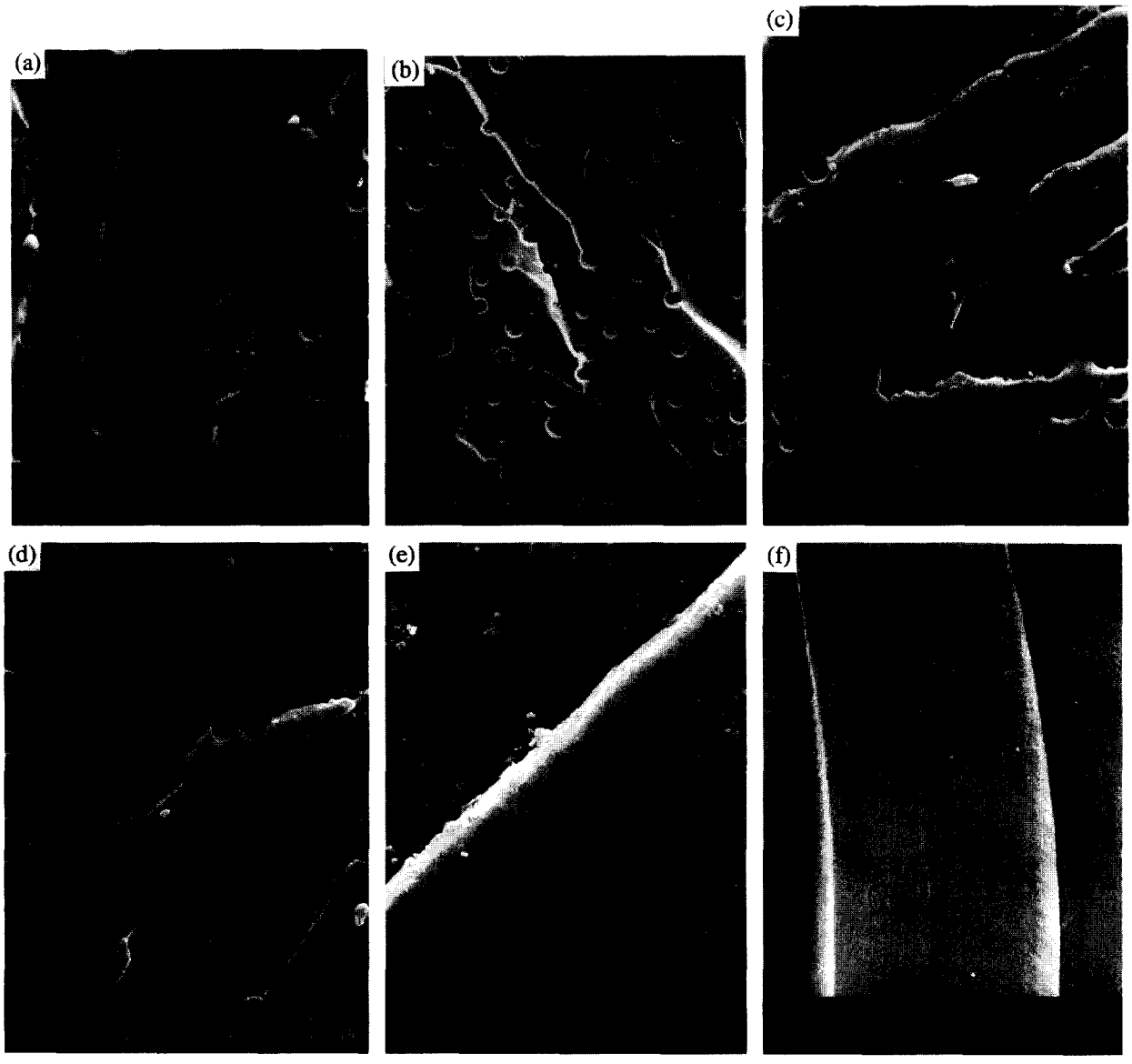

Figure 1 SEM micrographs of the etched fracture surfaces of the 10/100/134/x phenoxy/epoxy/DDS/CEMI blends: (a) $x = 0$; (b) $x = 0.10$; (c) $x = 0.15$; (d) $x = 0.15$; (e) $x = 0.3$; (f) $x = 0.5$

shows various degrees of phase separation. *Figure 1a* shows the morphology of the blend obtained from the slowest curing rate (no accelerator, gel time of 72 min), where the phenoxy phase exists as well-separated spherical particles with diameters ranging from 0.3 to 0.6 μm. This opaque blend has zero transmittance owing to phase separation and the different refractive indices of phenoxy and matrix epoxy. It is worth mentioning here that about one third of the etched holes have clean interfaces, while the rest show white, circular, diffuse zones between the epoxy matrix and the empty hole. These diffuse zones are probably transition zones of incomplete phase separation where both phenoxy and epoxy are present. A fraction of the phenoxy is etched out and leaves a porous epoxy network during the etching process.

The blend containing 0.1 phr accelerator (gel time of 62 min) (*Figure 1b*) and the blend containing no accelerator have dispersed phenoxy particles nearly identical in dimension and number, but the etched holes for the former blend are less well defined. Essentially all these holes are encircled by white rings owing to less complete phase separation in the blend containing 0.1 phr accelerator.

Figures 1c and *1d* show micrographs of a blend prepared at an intermediate curing rate (with 0.15 phr accelerator, gel time of 46 min); these micrographs were taken at different locations of the same specimen. *Figure 1c* shows one particular location of incomplete phase separation where the less well-formed phenoxy domains seem interconnected and significantly larger than those shown in *Figure 1a* and *1b*. *Figure 1d* shows a morphology with a rough surface, indicating the etching out of a small quantity of coagulated phenoxy at a very early stage of phase separation.

Figures 1e and *1f* show the solvent-etched single-phase morphologies of blends prepared at faster curing rates (gel times of 24 and 6 min, respectively). The linear phenoxy molecules are completely locked within the epoxy network at the molecular level and simply cannot be etched out of the cured network.

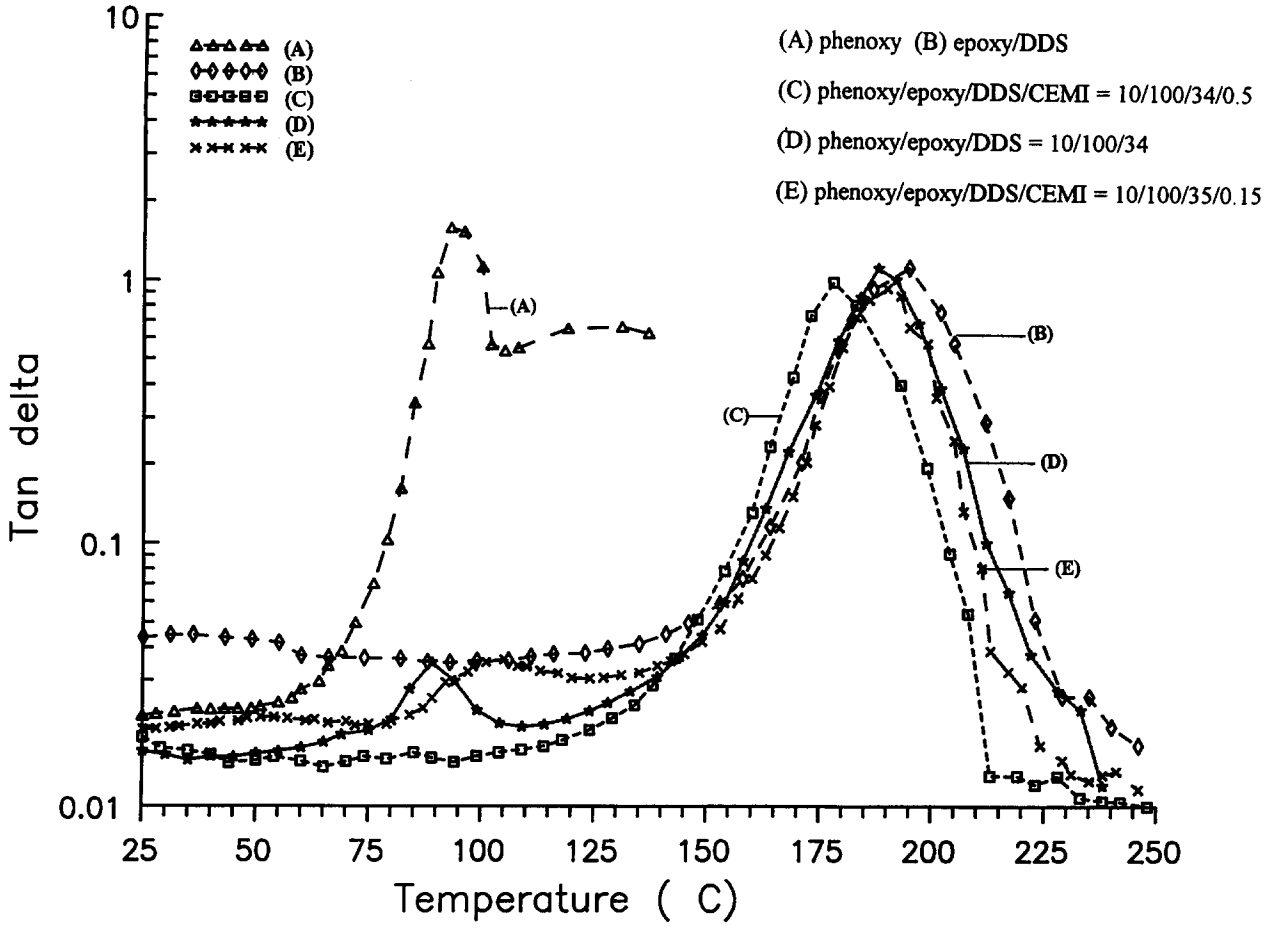

Figure 2 Dynamic mechanical spectra: (a) phenoxy; (b) epoxy/DDS; (c) 10/100/34/0.5 phenoxy/epoxy/DDS/CEMI; (d) 10/100/34 phenoxy/epoxy/DDS; (e) 10/100/35/0.15 phenoxy/epoxy/DDS/CEMI

Dynamic mechanical analyses

Dynamic mechanical properties can provide information on the microstructure of the cured resin. *Figure 2* and *Table 1* summarize the results of dynamic mechanical analyses for pure phenoxy, unmodified epoxy and phenoxy-modified epoxies. The epoxy T_g shifts to lower temperature and the magnitude of the shift increases with an increase in curing rate of the blend. The observed T_g shifts of the two single-phase, transparent blends relative to the unmodified epoxy are 10 and 16°C, respectively, which are close to the 11°C shift expected for a miscible blend according to the simple Fox equation[38]. Even for the opaque blends (0 and 0.1 phr CEMI) with two-phase morphologies, a T_g shift of 4–5°C has been observed. Such partial miscibility is probably a result of the structural similarity between phenoxy and the cured epoxy resin. The phenoxy T_g also shifts towards higher temperature with an increase in blend transparency. The translucent blend (0.15 phr CEMI) shows a T_g for the phenoxy phase that is increased by more than 10°C over the T_g of the pure phenoxy, and the Fox equation predicts about 10% of the epoxy dissolved in the phenoxy phase. The absence of the T_g peak of the phenoxy from the scans of the two transparent blends (0.3 and 0.5 phr CEMI) indicates that these blends are indeed homogeneous composites at the molecular level.

The microstructures of the blends as revealed by the dynamic viscoelasticity results are consistent with the morphologies observed by SEM and the corresponding levels of transparency. The data presented in our previous paper[31] indicated that the single-phase blend in this system is actually an immiscible blend in terms of thermodynamics. The thermodynamic driving force for the phenoxy to diffuse and separate from the phenoxy/epoxy solution is hindered by the high viscosity and/or the structural lock-in of the crosslinked epoxy network. The two transparent blends show a single T_g by differential scanning calorimetry (d.s.c.) and by dynamic mechanical analysis (d.m.a.), so one would usually consider them as miscible blends if neglecting the kinetic contribution. A single T_g as used in judging a miscible blend must be treated with caution, especially for the thermoplastic/thermoset blend system.

Phase separation mechanisms

The phase separation mechanisms and the resultant shape, size and size distribution of any rubber- or thermoplastic-modified thermoset are very complicated since both the thermodynamics and kinetics of the system have to be considered. For a non-crosslinkable polymer system, the morphology is mainly controlled by a thermodynamically reversible process. Unlike most binary thermoplastic blend systems, the molecular weight of the thermoset component and the resultant viscosity, T_g and crosslink density will change continuously with time once curing starts for any thermoplastic/thermoset system. Therefore, determination of the phase

separation mechanism for any thermoplastic/thermoset system strictly from thermodynamically derived rules is very difficult if not impossible. However, such rules derived for a thermoplastic/thermoplastic blend system can be used qualitatively to interpret the complex phase separation phenomenon.

Nucleation and growth (NG) in the metastable binodal region take place by localized fluctuations in concentration. The new phase starts from small nuclei which then proceed to grow and extend. Phase separation via the NG mechanism of the droplet/matrix type and the composition in the droplet is constant with only the droplet size changing with time.

Spinodal decomposition (SD) takes place in the unstable spinodal region with no sharp interfacial boundary in the initial stages of phase separation. Phase separation via the SD mechanism starts with a bicontinuous structure which gradually shifts to a droplet morphology of the minor component through breakdown of the bicontinuous structure.

For a thermoplastic/thermoset system, the binodal and spinodal curves will shift upwards (assuming an upper critical solution temperature (*UCST*) system as curing progresses, as shown in the schematic phase diagram of *Figure 3*. Therefore, NG and SD may both be involved in the phase separation mechanism, depending on the rate of phase separation. Verchere *et al.*[39] used a simple K ratio to describe the NG phase separation mechanism for a rubber-modified epoxy

$$K = (\text{phase separation rate})/(\text{polymerization rate}) \quad (5)$$

The polymerization rate represents the rate of upwards or downwards movement of the binodal and spinodal curves (*UCST* or lower critical solution temperature (*LCST*) system) which will determine the lifetime of a particular composition at a constant temperature within the binodal region. Analysis of the phase separation rate is rather complicated as it involves at least the thermodynamic driving force, interfacial tension and viscosity of the system. The kinetics of phase separation in the NG and SD mechanisms have been discussed in detail by Hsich[40]. The K value varies continuously with the progress of curing. The application of this simple K ratio concept is certainly not limited to the NG region of the phase diagram. If K is extremely high in the binodal region, equilibrium is instantaneously reached and the NG mode may be the only mode or the dominant mode of phase separation. Depending on K, a particular system may exhibit an NG mode, a dominant NG mode, a combination of NG and SD modes, a dominant SD mode or even no phase separation (at very low K). Phase separation by the NG mode was identified by Verchere *et al.*[39] for their rubber-modified epoxy system because of the low curing rate, low viscosity and low interfacial tension in the binodal region of the system (high K). A dominant SD mode[41] and even no phase separation[40] for other rubber-modified epoxy systems have been reported depending on the value of K.

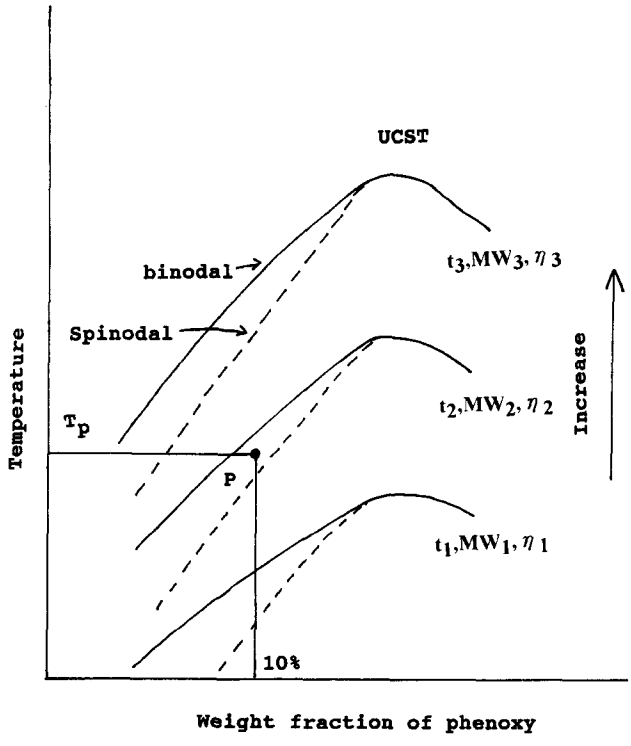

Figure 3 Schematic phase diagram illustrating the phase separation mechanisms of a thermoplastic/epoxy system

This phenoxy/epoxy system was prepared at constant curing temperature (135°C), fixed phenoxy molecular weight and constant weight fraction of phenoxy (10%). Point P in *Figure 3* represents the conditions used in this study with 10% phenoxy in the blend at a constant 135°C. Point P may fall in the binodal region (unless the composition is located at the critical point) then in the spinodal region following cure. The droplet morphologies of the slowly cured blends (higher K, *Figure 1a* and *1b*) are certainly insufficient and may be misleading in judging the mode of phase separation because both NG and SD modes can result in a similar droplet morphology. However, the translucent blend of intermediate curing rate (gel time of 46 min) shows signs of an interconnected structure (*Figure 1c*); therefore, the SD mode is probably the dominant mode of phase separation. Since the viscosity of this system is already very high at the beginning of phase separation, as mentioned elsewhere[31], the K value is not expected to be high enough in the binodal region to give an NG or dominant NG mode of phase separation. The single-phase, transparent blends (gel times of 24 and 6 min) of higher curing rates (*Figures 1e* and *1f*) have extremely low or near-zero K values (below a critical K value) and phase separation is hindered or completely halted owing to the high viscosity or high level of crosslinking of the system even though point P is located in the binodal or the spinodal region (*Figure 3*). As mentioned in the earlier section on d.m.a., the phenoxy phase in the translucent blend has a significantly higher content of the dissolved epoxy than the same phase in the opaque blend. This indicates that the composition of the phenoxy droplets varies with the progress of curing, and therefore the occurrence of an NG mechanism is less likely. In an NG mode of separation, the composition in the droplet is constant with only the droplet size changing with time.

In conclusion, the low to extremely low K values of this phenoxy/epoxy system result in an SD or dominant SD mode of phase separation for the opaque blends and no phase separation for the transparent blends. The translucent blend is the quenched morphology from

Table 2 Mechanical properties of the blends

Blend	Tensile strength (MPa)	Tensile modulus (GPa)	Compressive yield stress[a] (MPa)	K_{IC} (MPa m$^{1/2}$)	G_{IC} (J m^{-2})	Izod impact strength (J m^{-1})	δ_{tc} (μm)
Phenoxy	61	1.9	72				
Epoxy/DDS	73	3.0	133	0.75	158	29	1.2
Phenoxy/epoxy/DDS (0 phr CEMI)	71	2.9	126	1.06	325	41	2.6
Phenoxy/epoxy/DDS (0.1 phr CEMI)	71	2.8		1.08	350		
Phenoxy/epoxy/DDS (0.15 phr CEMI)	70	2.6		1.08	377		
Phenoxy/epoxy/DDS (0.3 phr CEMI)	68	2.5	118	1.11	414	45	3.5
Phenoxy/epoxy/DDS (0.5 phr CEMI)	65	2.2	109	1.20	550	48	5.0

[a] The compressive yield stress of phenoxy was taken from Union Carbide customer literature. The rest of the compressive yield stress data were obtained from our own tests based on an average of eight measurements for each sample

the initial stages of phase separation. The amount of the accelerator in the system serves to control the K value through the rate of curing. Kinetic control of the resultant morphologies, both homogeneous and inhomogeneous, by adding a small amount of accelerator to a rubber-modified epoxy has also been reported by Hsich[40].

Mechanical properties

The mechanical properties investigated in this study are summarized in *Table 2*. The tensile breaking strength and tensile modulus of the unmodified epoxy resin are only slightly higher than those of the two-phase opaque blends. However, the tensile moduli of the single-phase transparent blends decrease quite substantially with an increase in the amount of accelerator (or curing rate) in the blend. Since the unmodified epoxy and all the phenoxy/epoxy blends, both homogeneous and inhomogenous, fractured in uniaxial tensile testing prior to plastic yielding, the yield behaviour was examined by testing in uniaxial compression. The true compressive yield stress of phenoxy is substantially lower than that of the unmodified epoxy (72 compared to 133 MPa). The compressive yield stress of the opaque, inhomogeneous blend is very close to the value predicted by the rule of mixtures. The single-phase, transparent blend has a significantly lower yield stress than the opaque blend (109 compared to 126 MPa), even though both blends are almost identical in composition.

The behaviour of the yield stress in a binary blend is very complex, and many factors such as composition, degree of homogeneity, orientation, crystallinity, interfacial adhesion and testing conditions (rate, pressure and temperature) must all be taken into consideration. The situation becomes even more complicated in a thermoplastic/epoxy blend because the morphology and cross-linking density are also dependent on the curing rate. Variation of the curing temperature or addition of a different amount of accelerator can be used to control the curing rate and the final morphology. Curing at different temperatures alone can, in fact, lead to diverse network topologies. Unmodified and rubber-modified epoxies cured at higher temperature are apparently looser and more flexible, as indicated by the lower T_g, lower modulus, lower yield stress and higher fracture toughness[42]. This effect has been attributed to a higher free volume content in glasses cured at a higher rate[42]. It has also frequently been observed[43,44] that glasses obtained at a lower curing temperature (or a lower rate) have higher moduli in spite of their lower cross-linking densities. Most reports mention only the tensile modulus, while relatively few mention the yield stress in brittle epoxies because the more complicated compressive testing must be carried out. The yield stress and modulus are closely related in an almost linear relationship for the same polymeric materials and compositions and various testing conditions (temperature, rate and pressure) and structures (orientation, crystallinity and annealing)[45]. We can assume that the same trend in modulus and yield stress exists in this system. In the present study, a higher curing rate achieved by adding accelerator indeed has a similar effect to a higher curing temperature in terms of the resultant lower modulus, lower yield stress and higher fracture toughness of the final blend. The observed K_{IC} improvements in the phenoxy/epoxy blends over the unmodified epoxy are about 40–60% (*Table 2*), comparable to most other thermoplastic/epoxy systems previously reported[1]. The transparent blends have slightly higher K_{IC} than the opaque blends. The fracture toughness improvements in terms of G_{IC} (105–350%), shown in *Table 2*, are significantly higher than those in terms of K_{IC}, reflecting the substantial modulus difference in this system ($G_{IC} = K_{IC}^2/E$). The trend in the resultant impact strength is similar to that in G_{IC}, as shown in *Table 2*.

Toughening mechanism

The toughening mechanism of rubber-modified epoxies has been well documented, while that of thermoplastic-modified epoxies is less well understood. The phase separation phenomena of these two systems are very similar in many respects, both rubber and thermoplastic being miscible with the epoxy (and curing agent) even in the early stages of curing. Liquid rubbers containing reactive end-groups (carboxy or amino terminated) are more effective in toughening epoxies than the corresponding non-reactive rubbers[46]. Similar trends have also been observed for some thermoplastic-modified epoxies[10,12]. Rubber-modified epoxies can

increase in fracture toughness (K_{IC} or G_{IC}) by more than an order of magnitude over the unmodified counterparts, while the fracture toughness improvements in the thermoplastic-modified epoxies are considerably smaller[1]. The major difference between these two systems is that the dispersed rubber phase in the rubber-modified epoxy has a much lower T_g than the dispersed thermoplastic phase in the thermoplastic-modified epoxy. Owing to the soft nature of rubber (above T_g), the main toughness contributions in the rubber-modified epoxies come from the energy-dissipating deformations occurring in the vicinity of the crack tip, namely localized cavitation in the rubber caused by dilation near the crack tip and plastic shear yielding in the epoxy matrix. Other well-known mechanisms such as crack bridging, crack pinning, crack deflection, microcracking, crack bifurcation, rubber stretching, particle fracture and particle debonding may also contribute but are considered to be less essential to the total fracture toughness. However, the high modulus of the dispersed thermoplastic in the thermoplastic-modified epoxies does not allow for particle cavitation under triaxial tension, in contrast to rubber, and leads to significantly less plastic shear yielding in the epoxy matrix. Therefore, the less important mechanisms for rubber-modified epoxies now become significant for thermoplastic-modified epoxies. Several such failure modes may occur simultaneously depending on the type of particles and the matrix.

The K_{IC} values for rubber-modified epoxies are greater than the K_{IC} of the unmodified epoxy even at a temperature below the T_g of the rubbery second phase (e.g. 1.6 compared to 0.9 MN $m^{-2/3}$)[47]. This means that a similar toughness improvement to that measured for the thermoplastic-modified epoxy can still be measured for the rubber-modified epoxy when testing at a temperature where the rubber is in its glassy state.

Morphologies of fracture surfaces, typically from SEM micrographs, have frequently been used to identify or indicate the mode or modes of failure and then correlated with the obtained fracture toughness (K_{IC} or G_{IC}). Three-point bend and compact tension fracture mechanics have been most frequently used, and the fracture toughness K_{IC} (or G_{IC}) is then calculated from the maximum load as the critical load required for initiation of crack growth. Some of the above-mentioned fracture modes, such as rubber cavitation and plastic shear yielding, are known to be directly related to crack tip blunting and therefore the measured load at the onset of crack initiation. However, certain other modes, such as particle debonding, crack deflection and crack pinning, are considered to be less important or even give a negative effect in deciding the load for crack initiation, but certainly will contribute additional energy consumption during later crack propagation. Unless the double-cantilever beam (DCB) or tapered double-cantilever beam (TDCB) test is employed, any attempt to correlate directly the failure modes with the resultant fracture toughness based only on fracture surface observations may be misleading, and this viewpoint has rarely been addressed elsewhere.

Since the maximum load stress is often the only parameter other than the geometric parameter involved in determining the stress intensity factor (K_{IC}), the energy-dissipating mechanisms occurring prior to the onset of crack extension are the only mechanisms considered to be important. The energy sum from all these precrack energy-dissipating mechanisms can be considered as the energy required for crack tip blunting. The development of cavitation, voiding, shear deformation and the plastic zone near the crack tip raises the fracture toughness of the material because additional energy (or load) is required to compensate these loss energies for crack initiation to occur. The stored strain energy available for crack initiation should not now be taken as the input energy but rather as the difference between the input energy and the loss energy. A critical stored strain energy, input energy minus loss energy, has been found to dictate the onset of crack initiation in polycarbonates by varying the testing temperature, molecular weights and elastomer contents[48–50].

In this phenoxy/epoxy system, the relationship between yield stress and fracture toughness (G_{IC}) is very clear, as shown in *Table 2*. A lower yield stress tends to increase the size of the plastic zone near the crack tip, enhancing the crack tip blunting capability and resulting in toughness improvement. From a macroscopic point of view, the crack tip blunting capability is no doubt the major factor dictating the observed order of toughness in this study. In order to describe the effect of the crack tip blunting yield process on toughness, several models, such as those based on a critical plastic zone size[49], a critical crack tip opening displacement (CTOD)[51] or crack tip blunting[52], have been proposed. CTOD and crack tip blunting models are employed in this paper to describe the observed phenomena. Fracture occurs when the CTOD exceeds a critical value (δ_{tc}), and the critical CTOD is given by

$$\delta_{tc} = G_{IC}/\sigma_y \qquad (6)$$

where G_{IC} here is the critical strain energy release rate. Ideally, one would determine the fracture toughness

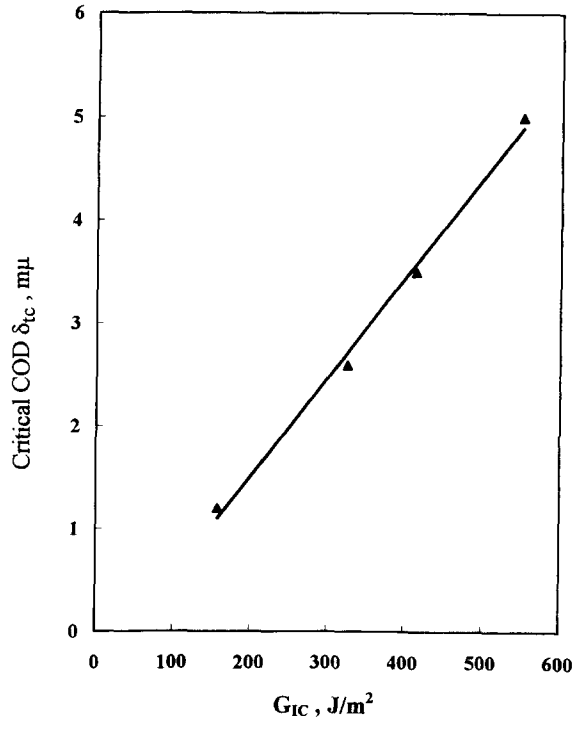

Figure 4 Relationship between G_{IC} and the calculated critical CTOD

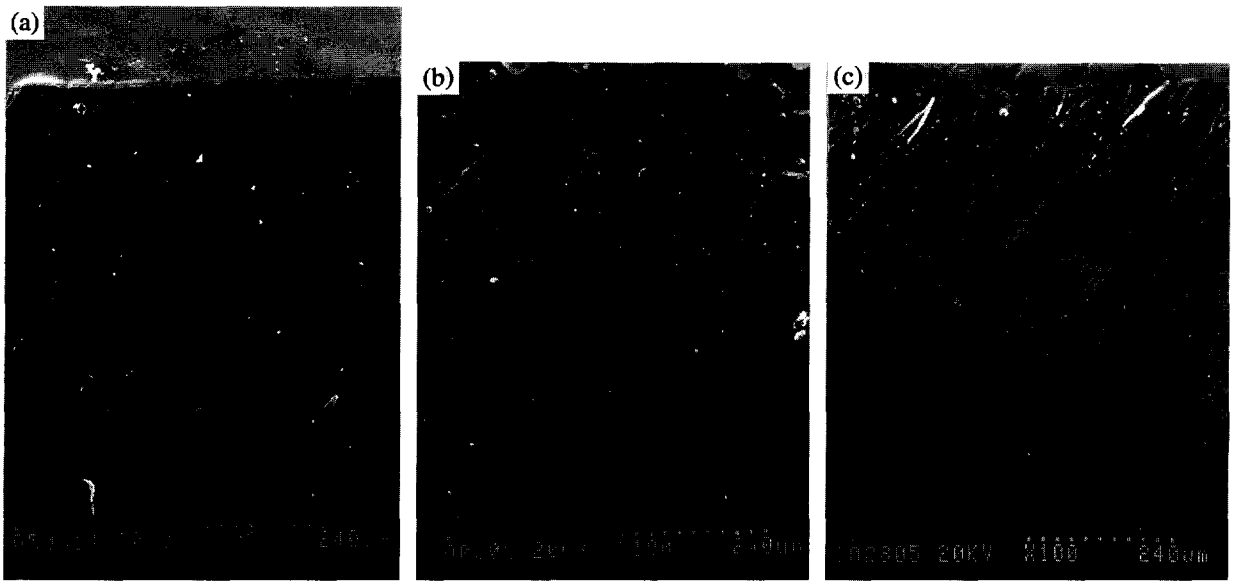

Figure 5 Morphologies of fracture surfaces for unmodified epoxy, an inhomogeneous blend and a homogeneous blend: (a) 100/34 epoxy/DDS; (b) 10/100/34 phenoxy/epoxy/DDS; (c) 10/100/35/0.5 phenoxy/epoxy/DDS/CEMI

(G_{IC}) by direct measurement of δ_{tc} and σ_y. The yield stress (σ_y) in equation (6) should correspond to the yield stress near the crack tip where high hydrostatic tensile stresses exist. The G_{IC} and the compressive yield stresses obtained experimentally were used to estimate the corresponding δ_{tc}, and the results are shown in *Table 2* and *Figure 4*. The calculated δ_{tc} increases with increasing G_{IC}, as would be expected. Without exception, the results from this study clearly indicate a definite correlation between the fracture toughness and the extent of plastic deformation in crack tip blunting. Greater crack tip blunting (greater δ_{tc}) will reduce the local stress concentration and the stored elastic energy required to strain the crack tip. Additional input energy (and stress) is needed to balance the loss energy resulting from plastic yield zone formation, and this is the foundation of the proposed crack tip blunting model.

For this phenoxy/epoxy system, the fracture surfaces of the single-phase blends are similar to the fracture surface of the unmodified epoxy. The fracture surfaces are smooth and featureless, apart from a few fine river markings emanating from the crack initiation region (*Figures 5a* and *5c*). Therefore, we can expect the same fracture mechanism for the homogeneous blends and the unmodified epoxy, except that the former have considerably lower yield stress and greater crack tip blunting prior to the onset of crack initiation. As mentioned earlier, the network structure of one homogeneous (*Figure 5c*, with the highest content of accelerator) is similar to that of the unmodified epoxy cured at higher temperature, which is apparently looser, more flexible and possesses a lower T_g, modulus and yield stress. The fracture toughness (K_{IC}) of an unmodified epoxy can be increased up to five times at the cost of reducing the T_g and elastic modulus simply by raising the curing temperature[42]. Similarly, the homogeneous blend containing 0.5 phr CEMI has the highest fracture toughness but also suffers the same disadvantages of having a lower T_g and lower modulus.

The fracture surfaces of the inhomogeneous blends (*Figures 1a* and *1b*) are similar to those of typical thermoplastic/epoxy or rubber/epoxy blends. The river markings have been reduced substantially in one inhomogeneous blend (*Figure 5b*). Overall, more surface roughness is found for the inhomogeneous blends than for the homogeneous blends. These results lead us to believe that greater energy dissipation may occur during crack propagation for the inhomogenous blends than for the homogeneous blends. The toughening mechanisms most mentioned in the literature for thermoplastic/epoxy blends such as crack bridging, crack pinning, crack deflection, crack tip bifurcation, microcracking, particle fracture and particle-induced shear yielding may be involved to different degrees for the inhomogeneous phenoxy/epoxy blends. Particle-induced shear yielding is probably the major mechanism that can contribute to the crack tip blunting prior to crack initiation and the localized energy dissipation during crack propagation. Unlike most reports of thermoplastic/epoxy systems which involve high modulus and high stress thermoplastics, the phenoxy used in this study has substantially lower modulus and yield stress. The modulus mismatch can create a stress concentration and initiate more yielding in the epoxy matrix. Therefore, this particle-induced shear-yielding mechanism, similar to that of the rubber particles in the rubber-modified epoxy, must be the key toughening mechanism. The lower yield stress also makes phenoxy particle yielding and tearing easier than for most high yield stress thermoplastics during fracture. The fracture surfaces (*Figure 1*) show evidence of a greater extent of localized shear yielding during crack propagation in the inhomogeneous blends relative to the homogeneous blends, thus supporting the above claim. We do not have any solid experimental evidence to show the presence of other mechanisms such as crack bridging, crack tip bifurcation, crack pinning or microcracking. However, under certain conditions, some of these mechanisms, such as crack pinning and microcracking, may actually induce earlier crack initiation and result in reduced toughness. If the microcracks formed in the region of highest triaxial tensile stress between the

plastic yield zone and elastic deformation zone are unstable, the stress concentration resulting from these microcracks may cause earlier crack initiation. Crack pinning by solid particles at the initial crack tip may interfere with crack tip shear yielding and also induce a stress concentration that leads to earlier crack initiation. Since the phenoxy particles have a lower yield stress than the epoxy matrix, they may enhance epoxy shear yielding near the crack tip region if the interfacial adhesion is strong. Crack bridging occurs only for good interfacial adhesion and it will certainly resist earlier crack initiation. It appears that these two types of toughening mechanisms, bridging and pinning, are interrelated, and it may be difficult to separate their contributions to the overall toughness. Both microcracking and crack pinning, if indeed present, will definitely increase the energy dissipation that occurs during crack propagation, but are unlikely to occur during crack tip blunting. Crack tip bifurcation is also expected to improve crack tip blunting slightly by diverting some energy into more than one crack front and delaying crack initiation. The polymer chains are highly strained at the crack tip region during blunting and reach a maximum strain at the onset of crack initiation when bond breakage occurs. Extensive chain flow occurs during the blunting process. An epoxy with a looser structure (greater free volume), lower yield stress or lower crosslinking density can allow a greater extent of chain flow, and results in better resistance towards crack initiation and higher toughness. An efficient toughening mechanism is one that is able to increase the blunting ability of the epoxy. We emphasize here that crack tip blunting is the most important factor in determining toughness, and all the above-mentioned micromechanisms are actually included in the blunting process.

Intrinsic toughness and toughenability of the epoxy matrix

Most rubber- and thermoplastic-toughened epoxies have a certain amount of free rubber or thermoplastic chains dissolved in the epoxy matrix. In the blend, the intrinsic properties of the epoxy have been changed and the intrinsic toughness of the epoxy is not that of the original, unmodified epoxy. The change in intrinsic toughness of the epoxy depends on the type and amount of dissolved chains. If the dissolved chains come from a flexible and ductile substance, like phenoxy in this study, the intrinsic toughness of the epoxy matrix will be increased. If the dissolved chains come from rigid and brittle substance, the intrinsic toughness of the epoxy may even decrease. In a similar study on PEI/epoxy blends, we found that the inhomogeneous blends were actually tougher than the corresponding homogeneous blends[18]. PEI is considered to be more rigid and more brittle then phenoxy, with significantly higher modulus and yield stress. In addition to the change in intrinsic toughness of the epoxy matrix, its toughenability can also be altered. The toughenability of the epoxy is expected to increase with the presence of dissolved thermoplastic chains to different degrees when a second phase (rubber or thermoplastic) is also present because the epoxy network becomes looser and more flexible. An effective rubber-toughened epoxy is believed to combine these changes in intrinsic toughness and toughenability in the epoxy matrix. The effect of a dissolved second component on intrinsic toughness for thermoplastic/thermoplastic blends has been discussed in detail elsewhere[53].

CONCLUSIONS

Transparent, homogeneous and opaque, inhomogeneous phenoxy/epoxy blends can be prepared through kinetic control of the curing rate by varying the amount of accelerator in the system. A simple K ratio has been adopted to explain the kinetically controlled phase separation phenomena. Spinodal decomposition is probably the dominant mechanism involved in the inhomogeneous systems. The K value varies continuously with the progress of curing, while the curing rate represents the rate of upwards (for an *UCST* system) or downwards (for a *LCST* system) movement for the binodal and spinodal curves. Depending on K and the curing rate, a particular system may display an NG mode, a dominant NG mode, a combination of NG and SD modes, or a dominant SD mode. A low K (or slow curing rate) in the binodal region of this phenoxy/epoxy system prevents an ND or dominant ND mode and favours the dominant SD mode for the inhomogeneous blends. An extremely low K (fast curing rate) in both the binodal and spinodal regions results in no phase separation and homogeneous blends.

Even for the inhomogeneous blends, a certain fraction of the added phenoxy is dissolved in the epoxy matrix, and the intrinsic properties of the epoxy matrix in the blend have therefore been changed. The intrinsic toughness of the epoxy matrix will increase on increasing the amount of dissolved phenoxy. The homogeneous blend that has the highest content of dissolved phenoxy in the epoxy matrix also possesses the highest fracture toughness. However, this homogeneous blend suffers the disadvantages of having lower T_g, modulus and yield stress. From the fracture surface morphologies, the homogeneous blends and the unmodified epoxy have similar fracture modes, except that the former have more shear yielding and higher fracture toughness.

A crack-blunting mechanism, where localized plastic deformation occurs at the crack tip prior to the onset of crack propagation, has been used to explain the fracture behaviour seen in this study. The degree of blunting caused by shear yielding around the crack tip is the most important factor in controlling the subsequent mode of crack growth and, to a large extent, the fracture toughness. The homogeneous blend containing the largest amount of dissolved phenoxy has the lowest yield stress, the highest degree of crack blunting before the onset of crack initiation and more localized shear yielding during crack propagation. The intrinsic toughness of the epoxy matrix of an inhomogeneous blend is also improved by the dissolved phenoxy. Moreover, the modulus mismatch between the dispersed phenoxy particles and the epoxy matrix induces additional localized shear yielding around the particles and raises toughness.

ACKNOWLEDGEMENT

The authors are grateful to the National Science Council, Republic of China, for financial support.

REFERENCES

1 Pearson, R. A. in 'Toughened Plastics', I (Eds C. K. Riew and A. J. Kinloch), Advances in Chemistry Series 233, American Chemical Society, Washington, DC, 1993, p. 405
2 Bucknall, C. B. and Partridge, I. K. *Polymer* 1983, **24**, 639
3 Bucknall, C. B. and Partridge, I. K. *Br. Polym. J.* 1983, **15**, 71
4 Bucknall, C. B. and Patridge, I. K. *Polym. Eng. Sci.* 1986, **26**, 54
5 Bucknall, C. B., Gomez, C. M. and Quintard, I. *Polymer* 1994, **35**, 353
6 Hedrick, J. C. and McGrath, J. E. *Polym. Bull.* 1985, **13**, 201
7 Kim, B. S., Chiba, T. and Inoue, T. *Polymer* 1995, **36**, 43
8 Raghava, R. S. *J. Polym. Sci., Polym. Phys. Edn* 1988, **26**, 65
9 Yamanaka, K. and Inoue, T. *Polymer* 1989, **30**, 662
10 Hedrick, J. L., Yilgor, I., Jurek, M., Hedrick, G. L., Wilkes, G. L. and McGrath, J. E. *Polymer* 1991, **32**, 2020
11 MacKinnon, A. J., Jenkins, S. D., McGrail, P. T. and Pethrick, R. A. *Macromolecules* 1992, **25**, 3493
12 Iijima, T., Hiraoka, H. and Tomoi, M. *J. Appl. Polym. Sci.* 1992, **45**, 709
13 Akay, M. and Cracknell, J. G. *J. Appl. Polym. Sci.* 1994, **52**, 663
14 Bucknall, C. B. and Gilbert, A. H. *Polymer* 1989, **30**, 213
15 Hourston, D. J., Lane, J. M. and MacBeath, N. A. *Polym. Int.* 1991, **26**, 17
16 Hourston, D. J. and Lane, J. M. *Polymer* 1992, **33**, 1379
17 Cho, J. B., Hwang, J. W., Cho, K., An, J. H. and Park, C. E. *Polymer* 1993, **34**, 4832
18 Wang, C. S., Teng, K. C. and Chang, F. C. in 'Proceedings of the 16th ROC Polymer Symposium', Taiwan, 1993, p. 303
19 Li, S. J., Hsu, B. L., Harris, F. W. and Cheng, Z. D. *Polym. Mater. Sci. Eng.* 1994, **70**, 51
20 Chen, M. C., Hourston, D. J. and Sun, W. B. *Eur. Polym. J.* 1995, **31**, 199
21 Pearson, R. A. and Yee, A. F. *Polym. Mater. Sci. Eng.* 1990, **63**, 311
22 Pearson, R. A. and Yee, A. F. *Polymer* 1993, **34**, 3658
23 Venderbosch, R. W., Nelissen, J. G. L., Meijer, H. E. H. and Lemstra, P. J. *Makromol. Chem. Symp.* 1993, **75**, 73
24 Kim, J. K. and Robertson, R. E. *Polym. Mater. Sci. Eng.* 1990, **63**, 301
25 Kim, J. K. and Robertson, R. E. *J. Mater. Sci.* 1992, **27**, 3000
26 Nichols, M. E. and Robertson, R. E. *J. Mater. Sci.* 1994, **29**, 5916
27 Cardwell, B. J. and Yee, A. F. *Polym. Mater. Sci. Eng.* 1994, **70**, 254
28 Hsia, H. C., Ma, C. C. M., Li, M. S., Li, Y. S. and Chen, D. S. *J. Appl. Polym. Sci.* 1994, **52**, 1137
29 Lu, M. L., Cheng, U. C. and Chang, F. C. in 'Proceedings of the Chinese Materials Science Conference', Taiwan, 1994, p. 36
30 Don, T. M., Yu, Y. and Bell, J. P. *Polym. Mater. Sci. Eng.* 1994, **70**, 49
31 Teng, K. C. and Chang, F. C. *Polymer* 1993, **34**, 4291
32 Iijima, T., Tochimoto, T. and Tomoi, M. *J. Appl. Polym. Sci.* 1991, **43**, 1685
33 Gomez, C. M. and Bucknall, C. B. *Polymer* 1993, **34**, 2111
34 Biolley, N., Pascal, T. and Sillion, B. *Polymer* 1994, **35**, 558
35 Kim, S. C. and Brown, H. R. *J. Mater. Sci.* 1987, **22**, 2589
36 Iijima, T., Arai, N., Takematsu, K. I., Fukuda, W. and Tomoi, M. *Eur. Polym. J.* 1992, **28**, 1539
37 Iijima, T., Sato, K., Fukuda, W. and Tomoi, M. *J. Appl. Polym. Sci.* 1993, **48**, 1859
38 Fox, T. G. *Bull. Am. Phys. Soc.* 1956, **1**, 35
39 Verchere, D., Sautereau, H., Pascault, J. P., Moschiar, S. M., Riccardi, C. C. and Williams, R. J. J. in 'Toughened Plastics I' (Eds C. K. Riew and A. J. Kinloch), Advances in Chemistry Series 233, American Chemical Society, Washington, DC, 1993, p. 335
40 Hsich, H. S. Y. *Polym. Eng. Sci.* 1990, **30**, 493
41 Yamanaka, K. and Inoue, T. *J. Mater. Sci.* 1990, **25**, 241
42 Lavita, G., Marchetti, A. and Butta, E. *Polymer* 1985, **26**, 1110
43 Findley, W. N. and Reed, R. M. *Polym. Eng. Sci.* 1977, **17**, 837
44 Enns, J. B. and Gillham, J. K. *J. Apply. Polym. Sci.* 1983, **28**, 31
45 Brown, N. in 'Failure of Plastics' (Eds W. Brostow and R. D. Corneliussen), Hanser, Munich, 1986, pp. 98–118
46 Huang, Y., Kinloch, A. J., Bertsch, R. J. and Siebert, A. R. in 'Toughened Plastics I' (Eds C. K. Riew and A. J. Kinloch), Advances in Chemistry Series 233, American Chemical Society, Washington, DC, 1993, pp. 189–210
47 Kinloch, A. J., Shaw, S. J., Tod, D. A. and Hunston, D. L. *Polymer* 1983, **24**, 1341
48 Chang, F. C. and Hsu, H. C. *J. Appl. Polym. Sci.* 1994, **52**, 1891
49 Chang, F. C. and Hsu, H. C. *J. Appl. Polym. Sci.* 1991, **43**, 1025
50 Chang, F. C. and Hsu, H. C. *J. Appl. Polym. Sci.* 1993, **47**, 2195
51 Kinloch, A. J., Shaw, S. J. and Hunston, D. L. *Polymer* 1983, **24**, 1355
52 Kinloch, A. J. and Williams, J. G. *J. Mater. Sci.* 1980, **15**, 987
53 Chang, F. C. and Hwu, Y. C. *Polym. Eng. Sci.* 1991, **31**, 1509